Dissolved cadmium in the Southern Ocean: Distribution, speciation, and relation to phosphate

O. Baars, W. Abouchami, S.J.G. Galer, Marie Boye, Peter Croot

Dissolved cadmium in the Southern Ocean: Distribution, speciation, and relation to phosphate

Oliver Baars,[1,a,]* Wafa Abouchami,[2,3] Stephen J. G. Galer,[2] Marie Boye,[4] and Peter L. Croot [1,b]

[1] Geomar, Kiel, Germany
[2] Max Planck Institute for Chemistry, Mainz, Germany
[3] Westfälische Wilhelms-Universität, Institut für Mineralogie, Münster, Germany
[4] Laboratoire des Sciences de l'Environnement Marin, Institut Universitaire Européen de la Mer (IUEM), Technopôle Brest Iroise, Plouzané, France

Abstract

We report isotope dilution analyses of dissolved cadmium (Cd) and electrochemical Cd speciation measurements in the Atlantic sector of the Southern Ocean. Bioavailable inorganic Cd is > 100 times higher in near-surface waters south of the Polar Front compared to the Subantarctic Zone because of upwelling and reduced complexation by organic Cd ligands. To trace local changes in the relation between Cd and P, we examine the deviations from a linear deep-water Cd vs. P relation (Cd*), and find that changes in Cd* coincide with the position of frontal systems and covary with primary productivity and total dissolved Mn and Fe concentrations. These covariations agree with potential local changes in phytoplankton Cd uptake rates, resulting from differences in the availability of Cd, Zn, Mn, and Fe. A band of negative Cd* values is associated with formation of Subantarctic Mode Water (SAMW) and Antarctic Intermediate Water (AAIW). In contrast to SAMW, which may export low Cd : P ratios from the Southern Ocean, the Cd : P ratios in AAIW increase by mixing with underlying Upper Circumpolar Deep Water before being exported from the Southern Ocean. Deep waters show constant Cd : P ratios, and both elements behave conservatively with end-member mixing between deep waters of the Weddell Gyre, the Antarctic Circumpolar Current, and inflowing North Atlantic Deep Water. Overall, our results support the hypothesis that the kink in the global Cd vs. P relation is largely caused by high Cd : P uptake ratios in the trace-nutrient–limited Southern Ocean.

Oceanic cadmium and phosphate distribution—Early studies on the oceanic distribution of cadmium (Cd) uncovered nutrient-type vertical profiles, whereby Cd is supplied to open-ocean surface waters via vertical mixing as atmospheric deposition is insignificant, and removed by physical adsorption and biological uptake by microorganisms (Bruland 1980). Cd is toxic for microalgae at elevated concentrations but may be taken up inadvertently (Brand et al. 1986). Laboratory studies show that at levels found in the open ocean, Cd can have a beneficial effect on phytoplankton by alleviating zinc (Zn) limitation stress, for example, by substitution for Zn in cambialistic carbonic anhydrases (Price and Morel 1990). The chemical speciation of Cd is an important factor controlling the biological availability and biogeochemical cycling of Cd, as $\sim$ 70–99% of Cd may be bound to strong organic ligands in surface waters (Bruland 1992; Sunda and Huntsman 2000; Ellwood 2004).

The vertical distribution of dissolved Cd tightly correlates with the macronutrient phosphate (P) in oceanic waters (de Baar et al. 1994). This correlation has been used alongside Cd : Ca ratios preserved in sedimentary foraminifera to reconstruct past changes in bottom-water P concentrations and ocean circulation (Boyle 1988). The relationship between Cd and P has been described by two intersecting lines, with a low slope part between 0 and ~ 1.3 μmol L^{-1} P and a steep slope and negative intercept part beyond this "kink" (Boyle 1988; Frew and Hunter 1992). The kink is believed to be formed by strong depletion of Cd with respect to P in the upper water column in high-nutrient, low-chlorophyll (HNLC) regions, the largest being the Southern Ocean (Cullen 2006), and by data from the North Atlantic with a peculiar low Cd vs. P slope (Yeats 1998). Several possible causes of this apparent contrast between the two oceanic regimes and other potential contributions to the observed kink have been proposed (Frew and Hunter 1992; Yeats 1998; Elderfield and Rickaby 2000) and compiled by Cullen (2006).

Aims of this study—The Southern Ocean is not only the globally largest HNLC region, it is also central to the global thermohaline circulation. The distributions of Cd and P have been previously studied in the Southern Ocean along transects at 6°W (Löscher et al. 1998), the Greenwich Meridian (Boye et al. 2012), and in the Weddell Sea (Westerlund and Öhman 1991; Nolting and Baar 1994), the Drake Passage (Martin et al. 1990), and the Ross Sea (Fitzwater et al. 2000). All of these studies show strong surface depletion of Cd with respect to P. In the Subantarctic Zone (SAZ) this leads to depletion of Cd while P is still present at elevated concentrations (Frew and Hunter 1992; Ellwood 2004). The strong depletion of Cd has been related to the specific biogeochemical environ-
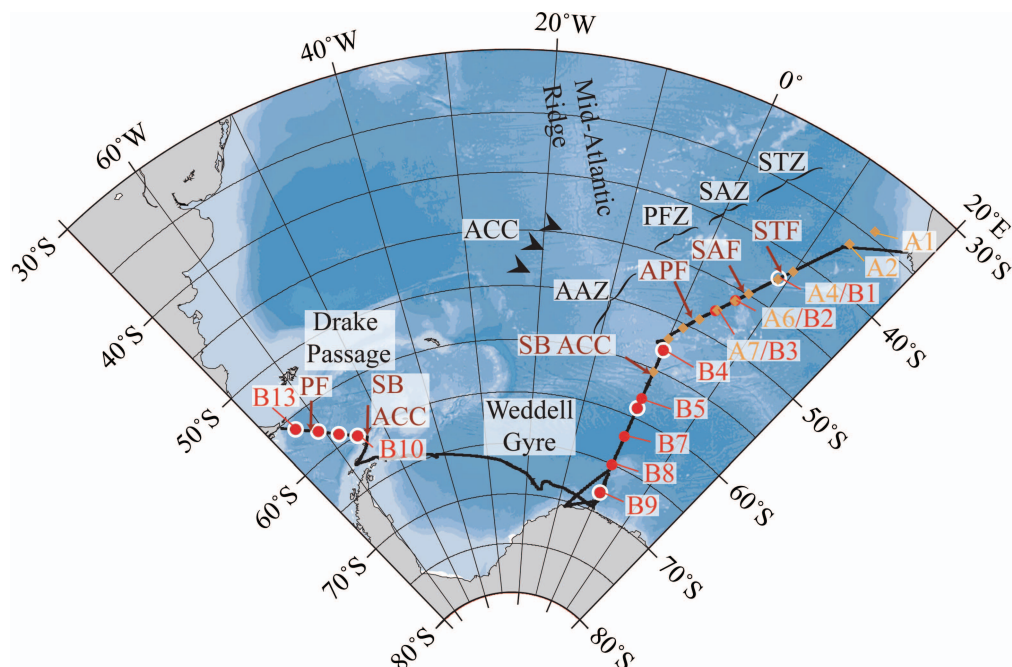
Fig. 1. Location of stations that were sampled for dissolved Cd during BGH (orange diamonds, A1–A11) and Z&D (red dots, B1–B13). The stations sampled for Cd speciation during Z&D are indicated with white circles. The domains are defined as: STZ = Subtropical Zone; ACC = Antarctic Circumpolar Current; SAZ = Subantarctic Zone; PFZ = Polar Frontal Zone; AAZ = Antarctic Zone; and the frontal systems as: STF = Subtropical Front; SAF = Subantarctic Front; APF = Antarctic Polar Front; SB ACC = Southern Boundary of the ACC.

ment and may include increased co-uptake of Cd with upregulated metal transporters, but evidence for factors controlling Cd uptake in the field is scarce (Sunda and Huntsman 2000; Cullen 2006). Moreover, apart from Antarctic coastal studies (Capodaglio et al. 1998) and one study in the SAZ (Ellwood 2004), to the best of our knowledge, there has been no study on Cd speciation in the Southern Ocean that can give information on the fraction of bioavailable Cd in this regime.

Previous studies have shown considerable variations in Cd : P ratios of deep waters, making it difficult to resolve the influence of deep-water export from the Southern Ocean, and highlight the need for high-precision and accurate Cd and P measurements to assess the true significance of the Cd vs. P relation in the worldwide ocean (Löscher et al. 1997). Yet it remains unknown if some of this variability reflects experimental uncertainty or true processes.

To further constrain the biogeochemical cycling of Cd, we present high-accuracy data for dissolved Cd distribution and organic speciation along the GEOTRACES cruise section "ANT24-3 Zero & Drake" (Fahrbach et al. 2011) in the Atlantic sector of the Southern Ocean conducted during the International Polar Year (IPY). The data set of dissolved Cd along the Greenwich Meridian is combined with published high-accuracy data for dissolved Cd along the quasi-synoptic IPY-GEOTRACES cruise section "Bonus-Goodhope" (Boye et al. 2012) to further include subantarctic and subtropical waters south of South Africa.

Both expeditions took place in the austral summer–autumn 2008 and had overlapping cruise tracks.

Methods

Note that, in the following, if not explicitly mentioned whether Cd or P concentrations refer to dissolved or particulate pools it is by default the dissolved phase (0.2 μm filtered samples). Unless otherwise indicated, Cd concentrations are always given in nmol L^{-1} and P concentrations in μmol L^{-1}. Cd : P ratios are given in nmol Cd : μmol P. Error margins comprise $\pm$ 1 standard deviation.

Station locations—Samples for analysis of dissolved Cd were collected during the IPY-GEOTRACES cruises Bonus-Goodhope (BGH; 08 February–24 March 2008) and ANT24-3 Zero & Drake (Z&D; 10 February–16 April 2008). Stations were partly overlapping to allow for intercalibration between both cruises. The organic speciation of Cd was investigated only during Z&D, including four stations along the Zero Meridian and four stations in the Drake Passage (Fig. 1). Details about the methods are given below.

Methods for dissolved Cd, hydrography, and macronutrient analyses—Methodologies during Z&D: Samples were retrieved with a trace-metal–clean rosette that was placed inside a clean laboratory container (Class-7) for subsampling (de Baar et al. 2008). Aliquots for determination

Table 1. Comparison of dissolved Cd results for the SAFe D2 intercalibration sample between the two different methods used during the BGH and the Z&D cruises ($\pm$ 1 standard deviation). The consensus values are given as of May 2013 using a density of 1.025 kg L^{-1} for conversion from per mass to per volume units. Details on collection and treatment of the intercalibration samples and latest consensus values are available on the GEOTRACES Web site (http://www.geotraces.org/science/intercalibration/322-standards-and-reference-materials).

Data set	SAFe D2
BGH	1034$\pm$15 pmol L^{-1} ($n=8$)
Z&D	1026$\pm$8 pmol L^{-1} ($n=5$)
Consensus value	1011$\pm$24 pmol L^{-1}

of dissolved Cd were filtered through 0.2 μm cartridges (Sartobran) into acid-cleaned low-density polyethylene (LDPE) bottles (Nalgene) and acidified to pH $<$ 2 with quartz-still–purified HCl. Nutrient samples were analyzed by the Royal Netherlands Institute for Sea Research using a TrAAcs 800 autoanalyzer (Bran & Luebbe) following standard methods described in Grasshoff et al. (1999). Temperature, salinity, dissolved oxygen, and fluorescence were recorded using Seabird™ sensors and validated using standard procedures (Grasshoff et al. 1999).

Sample preparation for isotope dilution–thermal ionization mass spectrometry (ID-TIMS) measurements of dissolved Cd involved further acidification to pH = 1 (HCl, Baseline Seastar™) and subsequent Cd extraction on an ion exchange column following established protocols (Schmitt et al. 2009; Abouchami et al. 2011). This method, initially developed for simultaneous determination of Cd concentration and Cd isotope composition in seawater, was slightly modified to allow faster processing of smaller volumes (10 mL) for concentration data only. Replicate determinations of Cd with a GEOTRACES intercalibration sample ("SAFe D2") were in excellent agreement with the consensus values (Table 1).

The complete data set will be available at the GEOTRACES International Data Assembly Centre (http://www.bodc.ac.uk/geotraces/).

Methodologies during BGH: Samples were retrieved with GO-FLO™ (General Oceanics) bottles attached to a Kevlar wire and closed using Teflon-coated messengers. The trace-metal–clean procedures during sampling and analysis have been described previously (Boye et al. 2012). The 0.2 μm filtered (Sartobran 300) aliquots for determination of dissolved Cd were, as for Z&D, stored in acid-cleaned LDPE bottles (Nalgene) but acidified to pH $<$ 2 with ultrapure HNO$_3$ (Merck). Dissolved reactive phosphate was analyzed manually by spectrophotometry (Murphy and Riley 1962). Silicate and nitrate were analyzed with an AAIII autoanalyzer (Bran & Luebbe; Treguer and Lecorre 1979).

Sample preparation for dissolved Cd involved solid-phase extraction on a Toyopearl AF-650M chelate resin column before analysis by isotope dilution–inductively coupled plasma mass spectrometry (Boye et al. 2012).

Method for Cd speciation measurements: Speciation measurements for dissolved Cd were performed at sea in an over-pressurized clean air container within 3 d after collection of the sample. The 0.2 μm filtered samples were stored in Teflon bottles before analysis. Analyses were done by anodic stripping voltammetry on a thin-film mercury electrode analogous to previous determinations of Zn speciation during Z&D (Baars and Croot 2011) but using a deposition potential of -0.85 V for Cd instead of -1.20 V for Zn. This potential was negative enough to quantitatively reduce inorganic Cd at the electrode while the stronger organic Cd complexes remained electroinactive. Analysis of the titration data was done by nonlinear regression using a one-ligand model (Eq. 1; Gerringa et al. 1995).

$$[CdL] = \frac{K'_{Cd'}[L]_T[Cd']}{1 + K'_{Cd'}[Cd']} \qquad (1)$$

In Eq. 1, [Cd$'$] is the inorganic (labile) Cd concentration that is directly related to the voltammetric peak current, [CdL] is the concentration of organic Cd complexes, calculated by difference between dissolved Cd and Cd$'$. Nonlinear regression with Eq. 1 yields K$'_{Cd'}$, the conditional stability constant of the organic Cd complexes with respect to inorganic Cd that is uncorrected for potential side reactions of the Cd ligands with competing cations. [L]$_T$ is the total concentration of organic Cd-binding ligands. Concentrations of free-solvated Cd (Cd^{2+}) were calculated assuming an inorganic side reaction coefficient $\alpha_{Cd'}$ = 34.7, which has been used in previous open-ocean Cd speciation studies (Bruland 1992; Ellwood 2004). The one-ligand model adequately describes the experimental data in this study in accordance with previous reports from the North Pacific and the SAZ (Bruland 1992; Ellwood 2004).

Results

Hydrographic setting and biogeochemical features—The frontal systems and water masses along the Zero Meridian and Drake Passage were identified by their characteristic temperature, salinity, oxygen, phosphate, and silicate properties. The hydrography along the Zero Meridian transect together with the station locations is shown in Fig. 2. Detailed descriptions of the hydrography and the biogeochemical features for the BGH cruise have been reported by Bown et al. (2011) and Le Moigne et al. (2013). An overview of the hydrography during Z&D is given in Fahrbach et al. (2011).

The first three stations close to South Africa (A1–A3) are in the Subtropical Zone (STZ) and characterized by Subtropical Surface Water with high salinity (S $>$ 34.5) and potential temperatures ($\theta > 10°$C). Surface waters south of the Subtropical Front and north of the Antarctic Polar Front (APF) are fresher (S $<$ 34.4) and colder (θ = 3–10°C) and combined under Subantarctic Surface Water. South of the APF, low temperatures ($\theta < 2.5°$C) and elevated silicate concentrations identify Antarctic Surface Water.

Below the surface, at the northern Sta. A2–A4, Subantarctic Mode Water (SAMW) is identified at 200–300 m
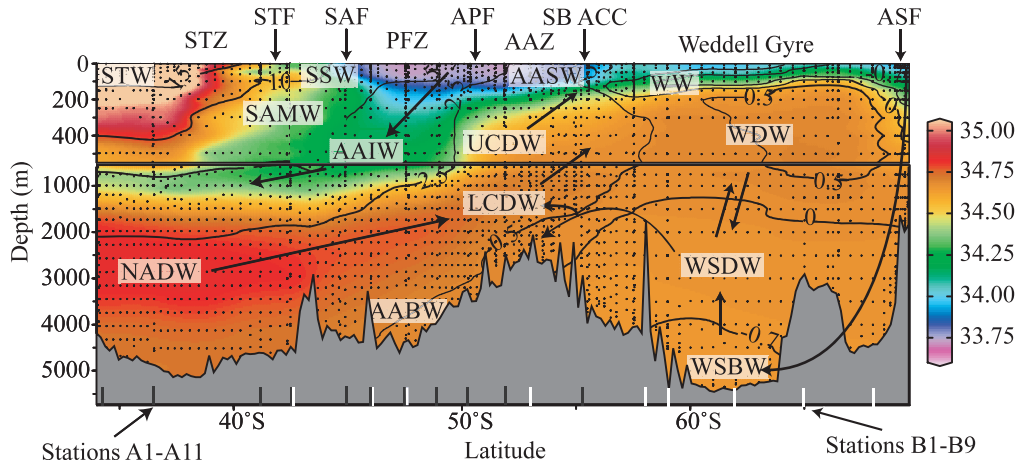
Fig. 2.   Salinity section with superimposed temperature contours along the Zero Meridian transect. The hydrography as described in the text is shown schematically. Lines at the bottom of the figure indicate the position of Sta. A1–A11 (black lines) and B1–B9 (white lines). All sections were created with Ocean Data View (Schlitzer 2013). AABW = Antarctic Bottom Water; AAIW = Antarctic Intermediate Water; AASW = Antarctic Surface Water; ASF = Antarctic Slope Front; LCDW = Lower Circumpolar Deep Water; NADW = North Atlantic Deep Water; SSW = Subantarctic Surface Water; STW = Subtropical Surface Water; UCDW = Upper Circumpolar Deep Water; WDW = Warm Deep Water; WSBW = Weddell Sea Bottom Water; WSDW = Weddell Sea Deep Water; WW = Winter Water.

by a negative Si* ($Si(OH)_4 - NO_3$) on a density surface between 26.8–27.0 (Sarmiento et al. 2004). Antarctic Intermediate Water (AAIW) of Indian Ocean origin is observed at depths between 500–1200 m at the northern stations (A1, A2) south of Africa and characterized by a subsurface salinity minimum (S = 34.4–34.6). A different variety of AAIW that is formed in the subantarctic region is found at Sta. A3–A7 and B2–B3 at depths between 500–800 m and distinguished by lower salinities (S < 34.3). The potential densities of AAIW samples are between 26.9 and 27.3. A layer of Upper Circumpolar Deep Water (UCDW), located below AAIW, is sampled at A2–A11, B2–B4, and B10–B13 with P maxima (P = 2.3–2.5 μmol L^{-1}), salinities between S = 34.39–34.67, and θ = 1.58–2.80°C. At higher latitudes (A11, B6, B7, and B9–B12), between 75–200 m, a layer of Winter Water (WW) is identified by a subsurface temperature minimum (θ = −1.8 to 0.4°C).

At greater depths, at the northern stations south of Africa, North Atlantic Deep Water (NADW) is found between 2000–3000 m and characterized by a P minimum (P = 1.8–2.0 μmol L^{-1}, θ = 1.3–2.2°C). NADW from A1–A4 is transported along the southwest African continental shelf and characterized by a characteristic salinity maximum (S > 34.79). NADW from higher latitude stations (A5–A7, B2) flows along the continental slope of South America before being injected into the Antarctic Circumpolar Current (ACC) in the southwestern Atlantic and shows less pronounced salinity maxima (S < 34.84). Lower Circumpolar Deep Water (LCDW) is below UCDW and sampled between 1000 and 3000 m, with P = 2.2–2.4 μmol L^{-1}. In the Weddell Gyre, below the temperature minimum of WW, is Warm Deep Water (WDW). Weddell Sea Deep Water (WSDW) is separated from WDW by a temperature drop (−0.7 < θ < 0°C) and collected from depths < 3500 m. The deepest water mass north of the Southern Boundary of the ACC is Antarctic Bottom Water

(AABW) with low potential temperatures (θ = 0.16–0.58°C) and salinities (S < 34.75). At higher latitudes, Weddell Sea Bottom Water (WSBW) samples are taken below WSDW from depths > 3500 m (θ < −0.7°C). In the Drake Passage, South Pacific Deep Water (SPDW) is found at 2000 m (B10, B11) and shows a local deep Si maximum with salinities between S = 34.70–34.71 and θ = 0.53–0.62°C.

The phytoplankton community in the Subtropical and Subantarctic Zones is dominated by nanoflagellates with significant numbers of dinoflagellates, particularly at A4 and B1 (Bown et al. 2011; Boye et al. 2012). The rest of the study area is diatom dominated, apart from B7 (62°S) where *Phaeocystis antarctica* is most abundant (Alderkamp et al. 2010). In this area, between 61–64°S, a bloom of *P. antarctica* was observed during the previous cruise (ANT24-2, December 2007–January 2008) after the spring sea ice retreat and was also visible by chlorophyll *a* estimations from remote sensing (Bluhm et al. 2011). During the time of this study, from late summer to autumn, the bloom had subsided and a diatom bloom is observed south of 65°S. Low algal abundance, as indicated by low chlorophyll *a* fluorescence, is found between 54–58°S along the Zero Meridian.

Total dissolved Cd—Interlaboratory comparison of dissolved Cd: The analysis results for the GEOTRACES trace-metal intercalibration sample "SAFe D2" with the two methods used during the BGH and Z&D cruises show excellent agreement between the methods and with the consensus value (Table 1). Dissolved Cd and P results for both cruises are further compared at two crossover stations at 46°S, 5°54′E (Sta. A6 and B2; Fig. 3A) and at 47°36′S, 4°18′E (Sta. A7 and B3; Fig. 3B). Both crossover stations were sampled individually at approximately the same location and occupied at about 2 week intervals during
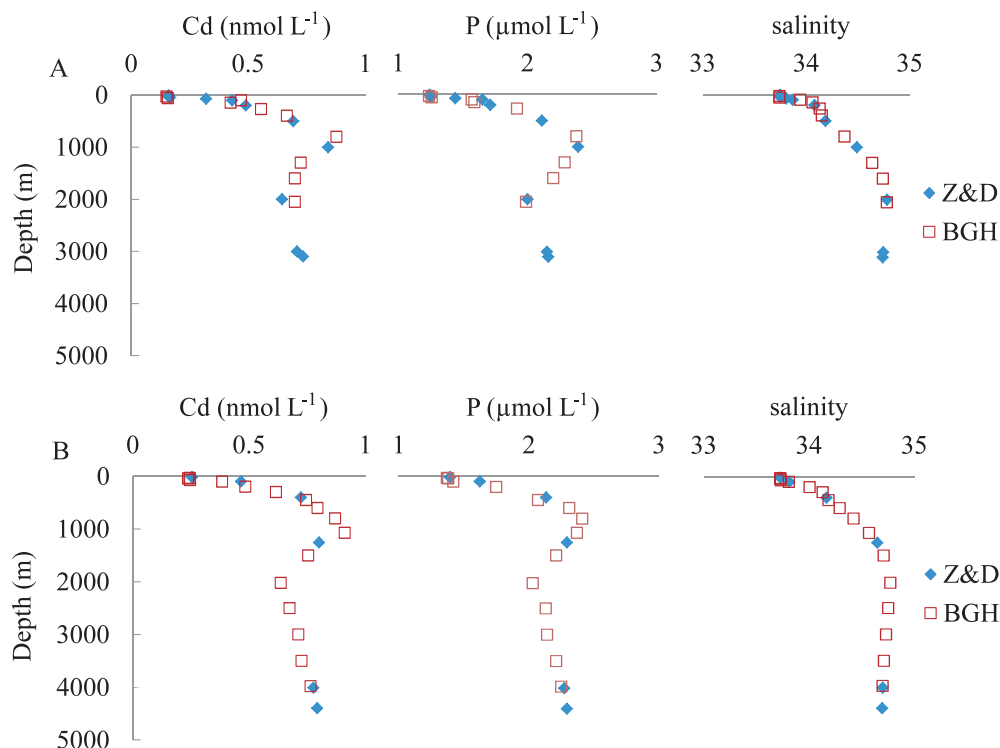
Fig. 3. Comparison of dissolved Cd, P, and salinity for two crossover stations sampled during the BGH and Z&D cruises at (A) 46°S, 5°54′E, Sta. A6 and B2; and (B) 47°36′S, 4°18′E, Sta. A7 and B3.

the BGH and Z&D cruises. The depth profiles are in excellent agreement.

Comparison with literature data from the Southern Ocean: We observe a strong linear correlation between Cd and P (Fig. 4) with slopes and intercepts in the range of values reported previously from this region (de Baar et al. 1994). The high accuracy and precision associated with the isotope dilution methods used here additionally allows to discern local changes in the relation between Cd and P in the upper and intermediate water column and reveals constant deep-water concentrations (Table 2) where considerable variation was reported in previous studies (Löscher et al. 1997). Moreover, the average deep-water Cd concentration of 0.79 ± 0.04 nmol L^{-1} in LCDW, AABW, WSBW, WSDW, and SPDW is higher than average literature values (between 0.61 and 0.67 nmol L^{-1}) reported in water masses of comparable salinity, temperature, and nutrient characteristics. This difference may be related to differences in analytical accuracy and precision. The relative standard deviation with the isotope dilution methods is < 2% for the deep-water Cd intercalibration sample SAFe D2 (Table 1). All published studies prior to IPY GEOTRACES had employed Cd detection by graphite furnace atomic absorption spectroscopy (GF-AAS), following a dithiocarbamate extraction–back extraction procedure. For these methods relative standard deviations have been reported in the range of 5–10%.

Further contributing to an underestimation of Cd with GF-AAS methods may be an incomplete recovery of Cd

during the extraction. In preliminary experiments for this study, we followed a dithiocarbamate liquid extraction protocol with GF-AAS detection (Grasshoff et al. 1999). Although our analysis of the SAFe D2 intercalibration sample using this method (1033 ± 17 pmol L^{-1}, $n = 2$) shows good agreement with the consensus value (1011 ± 24 pmol L^{-1}), the GF-AAS Cd concentrations for the Southern Ocean samples are ∼ 55% lower than those determined by ID-TIMS. Double extraction of some samples with this method confirms low and variable recoveries. Because the Cd concentrations measured by GF-AAS are close to the concentrations of inorganic Cd determined by anodic stripping voltammetry, we suspect that the incomplete recoveries may be connected to inert Cd species. An incomplete solvent extraction with ammonium pyrrolidine-dithiocarbamate has also previously been linked to non-exchangeable Cd species (Florence and Batley 1976). However, it should be noted that work performed during the European Iron Fertilization Experiment using HNO$_3$ instead of HCl for sample acidification and subsequent dithiocarbamate Cd extraction and GF-AAS measurement showed quantitative recoveries with no appreciable re-extraction blank (Croot et al. 2008), which suggests that the effect of inert natural Cd complexes may be minimized by decomposing them over time by the aid of the oxidizing acid.

In summary, the difference in the average deep-water concentrations between this and earlier studies can be largely explained by differences in analytical accuracy and precision, but we suspect that there may potentially also be
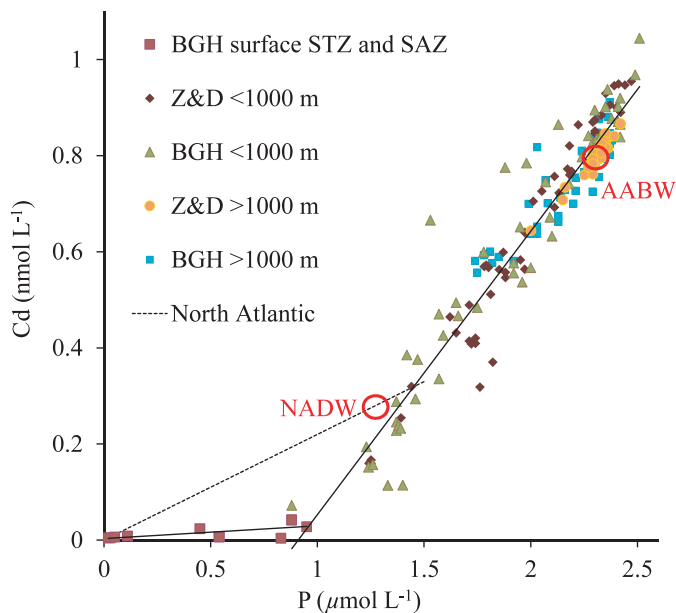
Fig. 4. Cd vs. P plot for all samples. Solid lines illustrate the kink. The lower slope part represents STZ and SAZ surface waters that were sampled during the BGH cruise. The best linear fit to the low slope part with zero intercept was: Cd (nmol L^{-1}) = (0.031 ± 0.006) × P (μmol L^{-1}); R^2 = 0.749. The steep slope part represents the remaining data set from both cruises with the following regression parameters: Cd (nmol L^{-1}) = (0.590 ± 0.012) × P (μmol L^{-1}) − (0.537 ± 0.026); R^2 = 0.924. The subset of all deep-water samples (> 1000 m) from the Z&D cruise closely followed a regression line with: Cd (nmol L^{-1}) = (0.540 ± 0.018) × P − (0.435 ± 0.038); R^2 = 0.926. This regression line was used for the calculation of Cd* (*see* text). The red circles show Cd and P concentrations in the source regions of AABW (this study) and NADW (Bruland and Franks 1983; Martin et al. 1993). The dotted line illustrates the Cd vs. P relation in the North Atlantic Ocean (de Baar et al. 1994).

an underestimation of Cd concentrations by GF-AAS methods relative to those obtained by the isotope dilution method depending on Cd speciation, sample storage, and extraction protocols.

Speciation of Cd—The northernmost Cd speciation Sta. B1 (42°20′S, 9°E) was in the SAZ, but no matching samples were collected for total dissolved Cd from this station during the Z&D cruise due to logistic reasons. However, Sta. A4 (42°28′S, 8°56′E), which was occupied during the BGH cruise 15 d later, was at approximately the same location and we use total dissolved Cd from A4 to estimate the organic complexation of Cd at B1. The good agreement between Cd depth profiles from both cruises at the intercalibration stations supports this approach (Fig. 3). Moreover, the near-surface Cd concentration at B1 has been determined by Abouchami et al. (2011; 10 m, Cd = 36 pmol L^{-1}). Because P concentrations at B1 decrease from the surface to a depth of 75 m, and because Cd concentrations covary with P, the range of near-surface Cd concentrations at B1 can be expected to be in good agreement with the measured values at A4 in this depth range (4–42 pmol L^{-1}). Using this approach, the highest

organic complexation of Cd (80–95%) is observed in the upper water column of B1, as a result of high ligand concentrations and complex stability constants in combination with depleted Cd in this area (Table 3). Note that this result is robust even if the estimation of total dissolved Cd from samples taken during the BGH cruise 15 d later should not be accurate for some surface-water samples. For example, the calculation for a sample at 25 m depth using the estimated total dissolved Cd from A4 (7 pmol L^{-1}) and the voltammetric speciation data from B1 yields L = 1.14 nmol L^{-1} and log K$'_{Cd'}$ = 10.05. By comparison, at a total dissolved Cd concentration of 1 pmol L^{-1}, these values would remain nearly constant (L = 1.13 nmol L^{-1}, log K$'_{Cd'}$ = 10.05), whereas increasing Cd significantly (Cd = 50 pmol L^{-1}) would result in only a slight increase of L and log K$'_{Cd'}$ (L = 1.18 nmol L^{-1}, log K$'_{Cd'}$ = 10.08). These results for Sta. B1 in the SAZ are in good agreement with a previous study of near-surface Cd speciation in the southeastern Pacific SAZ (Ellwood 2004).

The other stations analyzed for Cd speciation are located south of the APF and show a sharp contrast compared to the results of the SAZ. Here, the fraction of Cd bound to strong organic ligands is comparatively low in near-surface waters, and the inorganic Cd concentrations (Cd′) are about 100 times above those in the SAZ. This difference results from lower ligand concentrations and conditional stability constants while, at the same time, dissolved Cd is > 10 times higher due to upwelling deep water (Table 3). There is no significant difference in the speciation of Cd between the Drake Passage and the Zero Meridian, and no horizontal gradient in going polewards. In this region, we also do not detect significant differences in the speciation of Cd between surface and deep waters.

Discussion

Speciation of Cd—The highest Cd ligand concentration is found in the convergence zone between the subtropical and subantarctic domains (Sta. B1), where chlorophyll *a* is relatively high and nanoflagellates and dinoflagellates are abundant (Boye et al. 2012). Dinoflagellates and associated bacteria are known to be a source of organic ligands for copper (Croot et al. 2000) and may also produce ligands for Cd. In contrast, south of the APF, where ligand concentrations and strengths are lower, diatoms dominate the phytoplankton community. Some diatom species are known to effectively efflux Cd bound to the ligand phytochelatin under Cd stress (Lee et al. 1996; Wei and Ahner 2005). However, the absence of a difference in Cd complexation between surface and deep waters south of the APF suggests that if strong organic ligands were produced in surface waters, these were relatively unimportant for Cd complexation and could not be resolved from the measured ubiquitous ligand pool.

In coastal Antarctica, a time series study indicated that production of Cd ligands can be associated with phytoplankton blooms and that these ligands decay quickly after the bloom, on the order of days or weeks (Capodaglio et al. 1998). This would be consistent with organic Cd-binding ligands involving thiols, or other functional groups, which

Table 2. Comparison of Cd : P spot ratios, Cd, and P concentrations in different waters masses during this study ($\pm$ 1 standard deviation).

Water mass	Cd : P	$\pm$	Cd (nmol L^{-1})	$\pm$	P (μmol L^{-1})	$\pm$	*n*
Near-surface waters (Zero Meridian)							
STZ (P $<$ 0.9 μmol L^{-1})	0.130; 0.244		0.005; 0.007		0.02; 0.05		2
STZ, SAZ (P $>$ 0.9 μmol L^{-1})	0.005–0.013		0.004–0.009		0.11–0.83		3
PFZ	0.122–0.182		0.152–0.254		1.24–1.39		8
AAZ, Weddell Gyre	0.235–0.337		0.409–0.599		1.65–1.88		9
Intermediate waters							
SAMW	0.158; 0.210		0.194; 0.288		1.23; 1.37		2
AAIW	0.315	0.034	0.648	0.125	2.04	0.22	10
UCDW	0.365	0.020	0.865	0.066	2.37	0.07	25
WW	0.370	0.022	0.793	0.055	2.14	0.12	9
WDW	0.367	0.014	0.860	0.040	2.35	0.04	18
Deep waters							
NADW*	0.330	0.023	0.643	0.070	1.95	0.14	16
LCDW	0.350	0.015	0.797	0.047	2.28	0.05	13
AABW	0.344	0.015	0.777	0.054	2.26	0.10	11
WSBW	0.347	0.006	0.799	0.018	2.30	0.02	4
WSDW	0.347	0.004	0.806	0.013	2.32	0.02	11
SPDW	0.332; 0.343		0.761; 0.790		2.29; 2.30		2

* Inflowing "recent" NADW in the study area.

are known to be oxidized or metabolized rapidly (Laglera and van den Berg 2006). Considering that our sampling took place at the end of the growth season, the low surface ligand concentrations recorded south of the APF were conceivably a result of both a fast decay of ligand pools that may be produced during the summer bloom and low production rates at the time of our study. The high vertical water exchange south of the APF further acts to dilute surface signals.

Overall, our results suggest that during the time of this study, upwelling deep waters controlled the distribution of organic Cd ligands in near-surface waters south of the APF. Marine humic matter as refractory organic matter appears to be only a source of weak ligands for Cd in seawater with stability constants of log K′ = 6.1 (Grzybowski 2000), i.e., orders of magnitude below the stability constants of ligands detected in this study. Other potential sources of deep-water Cd ligands include hydrothermal vents (Sander et al. 2007) or sediments (Skrabal et al. 2006) as has been observed for Cu. Further studies are needed to investigate whether the deep-water Cd ligands might originate in deep waters or if they are mainly derived from export of compounds produced in near-surface waters.

The overall Cd–P relationship in the Southern Ocean—We use three complementary approaches to investigate the Cd–P relation in this study:

(1) Plots of Cd vs. P, which illustrate the overall relation between both elements. In the STZ and SAZ, Cd is depleted at P $<$ 0.9 μmol L^{-1} and these waters make up the low slope (0.031 $\pm$ 0.006) part in the Cd vs. P plot. Farther south, Cd and P increase due to upwelling and above this P concentration there is a strong linear correlation throughout the study area

(Fig. 4). The steep slope (0.59 $\pm$ 0.01 nmol Cd : μmol P) and the negative intercept (-0.54 ± 0.03 nmol L^{-1} Cd) are linked to a preferential incorporation of Cd over P into biogenic particles at the surface and remineralization in deeper waters.

(2) Cd : P spot ratios are useful to compare different water bodies within the study area with reported ratios in the global ocean (Table 2). Because of the preferential removal of Cd from the dissolved phase near the surface, the dissolved Cd : P spot ratios are always lowest in near-surface samples and increase together with Cd and P as a result of remineralization. Note that, in the following, Cd : P will always indicate spot ratios of dissolved Cd : P, whereas the Cd vs. P slope is obtained by linear regression with a set of samples.

(3) Cd*, which we define as the deviation of measured Cd from the deep-water Cd vs. P regression line: Cd* = Cd − (0.540 × P − 0.435) (Figs. 5, 6). Data points with positive Cd* are located "above" the deep-water regression line, data points with negative Cd* are below. Mapping the distribution of Cd* allows to sensitively discern local changes in the Cd vs. P relation. Similar to the concept of Si* (Sarmiento et al. 2004, 2007), Cd* remains constant if sources (remineralization) and sinks (uptake) of Cd and P introduce or remove these elements at the mean deep-water ratio of 0.540 (slope) while the constant of −0.435 (intercept) fixes the deep-water Cd* in the study area to zero. Cd* increases if remineralization occurs at a ratio of Cd : P $>$ 0.540 or if uptake occurs at a ratio of Cd : P $<$ 0.540 and vice versa. The distribution of Cd* recorded in this study shows local changes that

Table 3. Cd speciation results and comparison with other worldwide Cd speciation data sets.

Region	Depth (m)	Cd (pmol L⁻¹)	L (nmol L⁻¹)	log K'_Cd'	Cd' (pmol L⁻¹)	CdL (%)	Reference
Narragansett Bay (Rhode Island)	Surface	26–80	3.7 (3.6–3.8)	9.0 (9.0–9.2)	69–243	73–83	Kozelka and Bruland 1998
North Pacific	<200	2–44	0.07 (0.023–0.105)	10.4 (10.0–10.8)	0.70–763	11–80	Bruland 1992
	200–600	75–780	—	—	76–767	—	Bruland 1992
SAZ East Pacific	<80	4–51	1.5 (1.0–2.1)	10.3 (9.8–11.0)	0.2–1.3	87–99	Ellwood 2004
SAZ Atlantic Ocean	<80	4–42	0.9 (0.8–1.1)	10.2 (9.9–10.4)	0.2–3.1	86–96	This study
	200–500	194–533	1.1 (1.0–1.2)	10.4 (10.3–10.5)	7–36	93–97	This study
	4350	750	0.8	9.7	303	60	
Antarctic Ocean	0–100	310–845	0.80 (0.61–1.08)	9.4 (9.0–9.6)	139–451	45–75	This study
	>100	625–930	0.77 (0.55–1.05)	9.4 (9.0–9.7)	278–521	35–62	
Coastal Antarctica	0–250	60–990	0–2.2*	9.1–9.9	10–1110	0–92	Capodaglio et al. 1998

* Depleted below 50 m, dependent on sampling time (no ligand in November, production with beginning of December).

coincide with the positions of oceanographic fronts (Fig. 6). Corresponding changes in uptake and remineralization of Cd and P in surface waters are discussed in the section on the Cd–P relationship in surface waters. The formation of AAIW and SAMW is also visible in the Cd* section illustrating transport of negative Cd* values from Polar Frontal Zone (PFZ) surface waters to intermediate depths.

Conservative behavior of Cd and P in deep waters—Deep waters (> 1000 m) from Z&D match a linear Cd vs. P regression line most closely (Fig. 4). At the same time, an inverse correlation for both Cd and P with salinity is observed in deep-water masses of recent NADW and in the deep ACC along the Zero Meridian (NADW, AABW, LCDW; Fig. 7). The Cd data points are distributed along a common regression line with slightly larger residuals for BGH data ($R^2 = 0.80$) and very small residuals for Z&D data ($R^2 = 0.97$), indicating that the Cd vs. P relationship in these waters is controlled by mixing between the low-salinity, high-Cd, high-P ACC water body with inflowing recent high-salinity, low-Cd, low-P NADW. A close Cd and P vs. salinity correlation is also found in the deep Weddell Gyre waters—WSDW and WSBW—but in contrast to the deep ACC the data points are distributed along a positive slope. WSBW is fresher and colder than the overlying WSDW and formed by sinking of Coastal and Continental Shelf Water. As for the deep ACC waters, the correlation in the Weddell Gyre indicates conservative behavior but in this case the young and fresh WSBW end-member contains lower Cd and P than older and more saline overlying WSDW. Overall, the deep-water Cd and P relation in the study area behaves conservatively with no significant local sources or sinks for Cd or P.

Linear relationships between Cd, P, and salinity have been reported previously from the deep Central and South Atlantic (Yeats et al. 1995), and extrapolation of this reported linear relation to the salinity of AABW (S = 34.67) predicts a Cd : P ratio of 0.345 in agreement with our measured value of 0.348 ± 0.006 ($n = 7$) for AABW (S = 34.68–34.70). Extrapolation of the linear deep-water Cd vs. P relation from Z&D to P concentrations of NADW ($\sim 1.3 \mu mol L^{-1}$) yields a Cd concentration of 0.29 nmol L⁻¹ and a Cd : P ratio of 0.22 for NADW, consistent with measurements in the deep North Atlantic (Bruland and Franks 1983; Martin et al. 1993; Fig. 4). The good agreement of predictions based on linear Cd vs. salinity and Cd vs. P relationships with measurements of Cd and P in this study for the Southern Ocean and previous studies for the deep Atlantic Ocean suggests that the deep-water Cd vs. P relation throughout the Atlantic Ocean may be reasonably described by mixing between NADW and AABW end-members without strong decoupling between both elements in the deep Atlantic Ocean.

Intermediate waters and export of Cd–P properties with AAIW or SAMW—The lowest dissolved Cd : P ratios are always found in near-surface waters, which reflects preferential removal of Cd from the dissolved phase by
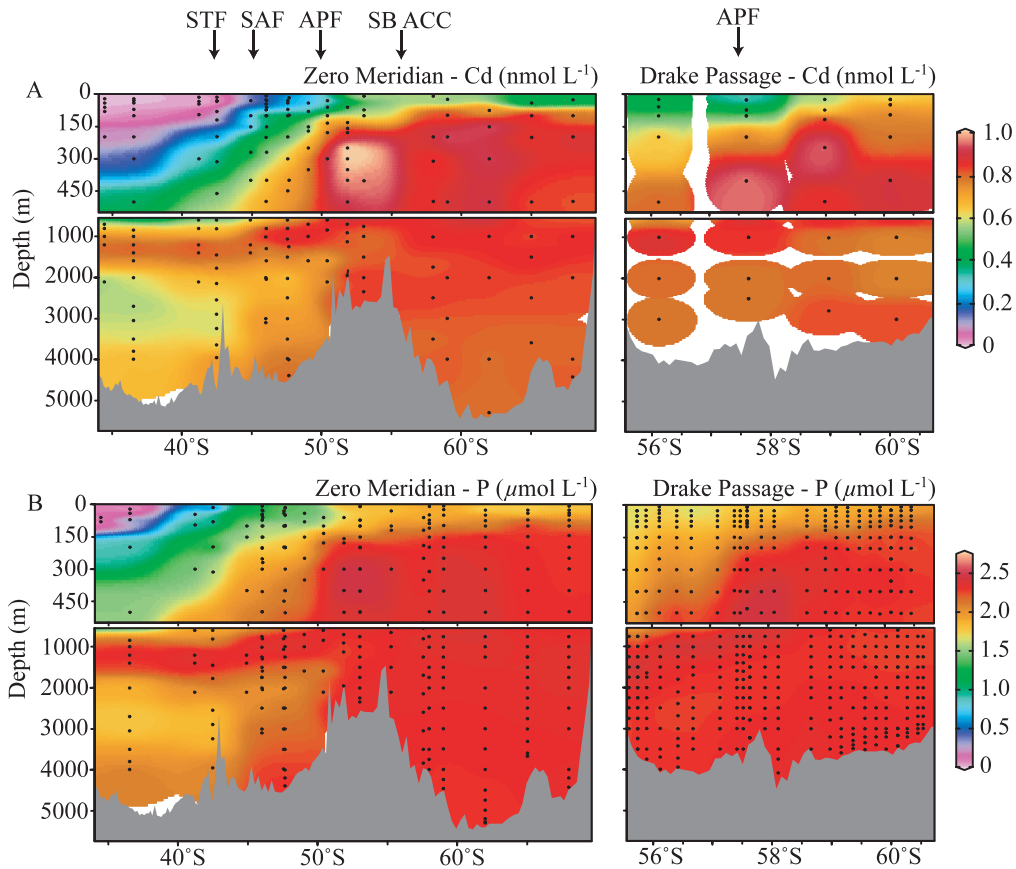
Fig. 5. Sections of (A) Cd and (B) P along the Zero Meridian and Drake Passage transects.

incorporation into biogenic particles. Upwelling deep water transports high dissolved Cd:P back to the surface and Cd:P ratios increase southward as the SAF and APF are crossed along the Zero Meridian. South of the APF, continuous upwelling of deep water holds surface-water concentrations at a high level while remineralization of biogenic particles with high Cd:P ratios from the surface can act to increase the preformed Cd:P ratio and result in the highest observed Cd:P ratios in waters south of the

APF at intermediate depth (WW, UCDW, and WDW; Table 2). Intermediate waters south of the APF show also the most positive Cd* signatures (Fig. 6), in agreement with high near-surface Cd:P uptake ratios (> 0.54) and remineralization at intermediate depth.

AAIW and SAMW are intermediate-depth water masses that are formed by sinking of surface waters in the PFZ and SAF region and flow northwards into lower latitudes of the global ocean. The formation of AAIW and SAMW is
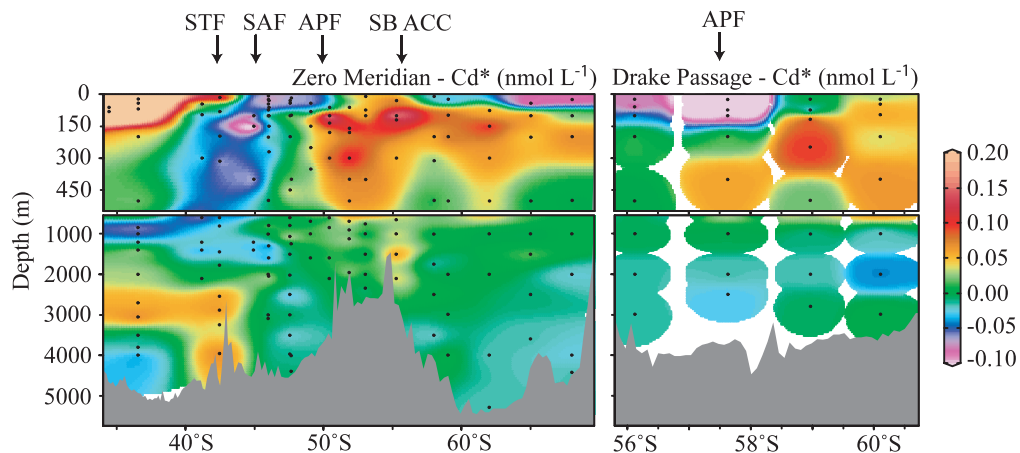

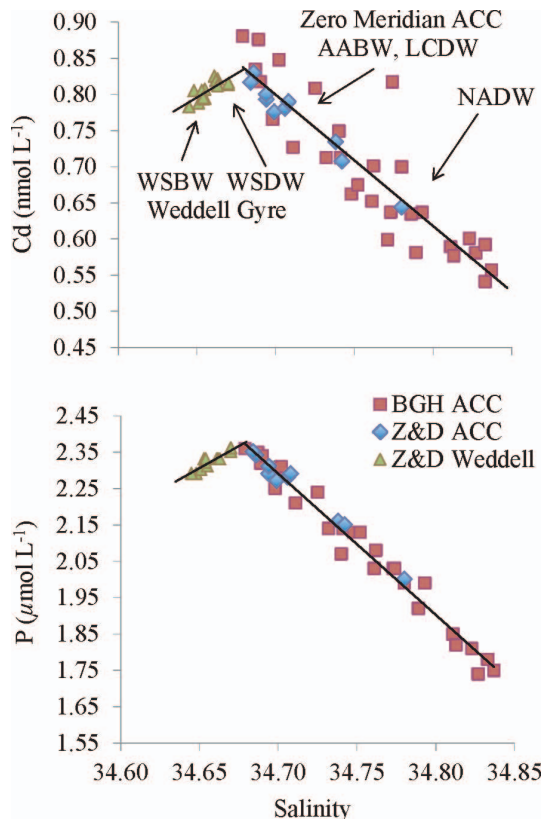Fig. 6. Distribution of Cd* = Cd − (0.540 × P − 0.435) along the Zero Meridian and Drake Passage.

Fig. 7.   Cd and P vs. salinity in deep-water masses (> 1000 m) of the ACC along the Zero Meridian compared to the deep Weddell Gyre.

visible in the Cd* section as a transport of negative Cd* values from surface waters to intermediate depths (Fig. 6). In the source region of AAIW formation (Sta. A8), the Cd : P ratio near the surface (40–80 m) is 0.167 while the Cd : P ratios in AAIW (identified between Sta. A1–B3 in depths of 500–1200 m) range between 0.26 and 0.36 with an average of 0.32 (Table 2). The Cd : P ratios in the overlying SAMW identified at A3 (300 m) and A4 (200 m) are 0.21 and 0.16. Strong correlations between Cd, P, and Cd : P with potential densities (σ) in AAIW (σ = 26.9–27.3; Cd [nmol L^{-1}] = 0.993 × σ − 26.369; R^2 = 0.94; n = 28; P [μmol L^{-1}] = 1.840 × σ − 47.993; R^2 = 0.96; n = 14; and Cd : P = 0.313 × σ − 8.208; R^2 = 0.89; n = 14) suggest that mixing with underlying UCDW (σ > 27.4–27.7, Cd : P = 0.35) can increase the dissolved Cd : P ratios within AAIW. Because Cd is essentially depleted north of the SAF but retains high P concentrations, the Cd : P uptake ratios are necessarily low (*see* section on the Cd–P relationship in surface waters) and remineralization of particulate organic matter formed in this region cannot contribute to an increase of Cd : P in AAIW or SAMW.

The export of low surface Cd : P ratios by AAIW into intermediate waters of the global ocean has been suggested to contribute to the observed kink in the global Cd vs. P relationship. This hypothesis was based on measured low Cd : P ratios in AAIW south of New Zealand (Cd : P = 0.22–0.23; Frew and Hunter 1992, 1995). However, higher

Cd : P ratios (Cd : P = 0.28) have been recorded in AAIW in the South Atlantic (Yeats et al. 1995). Our data indicate that the Cd : P ratio in AAIW is increased by mixing with underlying UCDW before it is exported towards lower latitudes. The situation may be different for SAMW, which has no direct contact to UCDW. A previously reported global Cd vs. P relationship on the density surface corresponding to the lower edge of SAMW (σ = 27.0) showed a low slope and an intercept close to zero compared to a steep slope and a negative intercept in AAIW (Yeats 1998). Because of the zero intercept, the slope (0.25) represented also dissolved Cd : P spot ratios in SAMW, which is close to the Cd : P ratio we find in young SAMW (Cd : P = 0.21; Sta. A3 at 300 m). The absence of mixing between SAMW with high Cd : P waters, such as UCDW, could provide an explanation for the difference in the Cd vs. P relationship between SAMW and AAIW in the global ocean that has been reported by Yeats (1998).

The Cd–P relationship in surface waters—Changes in near-surface Cd*: The lowest dissolved Cd : P ratios were found in surface waters of the SAZ (Table 2). The increase in Cd : P ratios to the north of the SAZ can be explained by the depletion of Cd at P < 0.9 μmol L^{-1}, which prevented further preferential removal of Cd with respect to P. On the other hand, the increase in Cd : P ratios to the south can be explained by upwelling of high Cd : P deep waters, consistent with high preferential Cd particle incorporation in the surface Southern Ocean and remineralization at intermediate depth. Incorporation of Cd into particles is principally through biological uptake as adsorption to biogenic matter is considered to be minor based on previous studies in mesocosms (Kremling et al. 1978; Kuiper 1981) and the open ocean (Yang et al. 2012), although a study in the English Channel suggested that Cd adsorption to bacterial surfaces may be important during phytoplankton blooms (Dixon et al. 2006).

To better understand what might cause high Cd : P uptake ratios, we look at regional changes of Cd* in near-surface waters together with several other parameters of interest (Fig. 8). Cd* increases if Cd and P are removed from the water column with Cd : P < 0.540 or if they are added with Cd : P > 0.540.

Notably, along the Zero Meridian, changes in Cd* coincide with the position of the frontal systems and covary with biological activity and total dissolved Mn and Fe concentrations. In particular, negative Cd* is found in the more productive waters to the north, in the PFZ, and to the south, in the southern Weddell Gyre, whereas positive Cd* occurs in the Antarctic Zone (AAZ), coinciding with low primary productivity (~ 50–59°S). Along the Drake Passage, the lowest Cd* is found in the vicinity of the APF (B12) which is known to be an area of intense biological activity (Pakhomov et al. 2000). The low Cd* values are consistent with high Cd : P uptake ratios in productive surface waters, whereas vertical water exchange south of the APF acts to increase Cd* (Fig. 6) in regions of low primary productivity.

Elevated biological activity is also detected at the southernmost station along the Drake Passage, but here
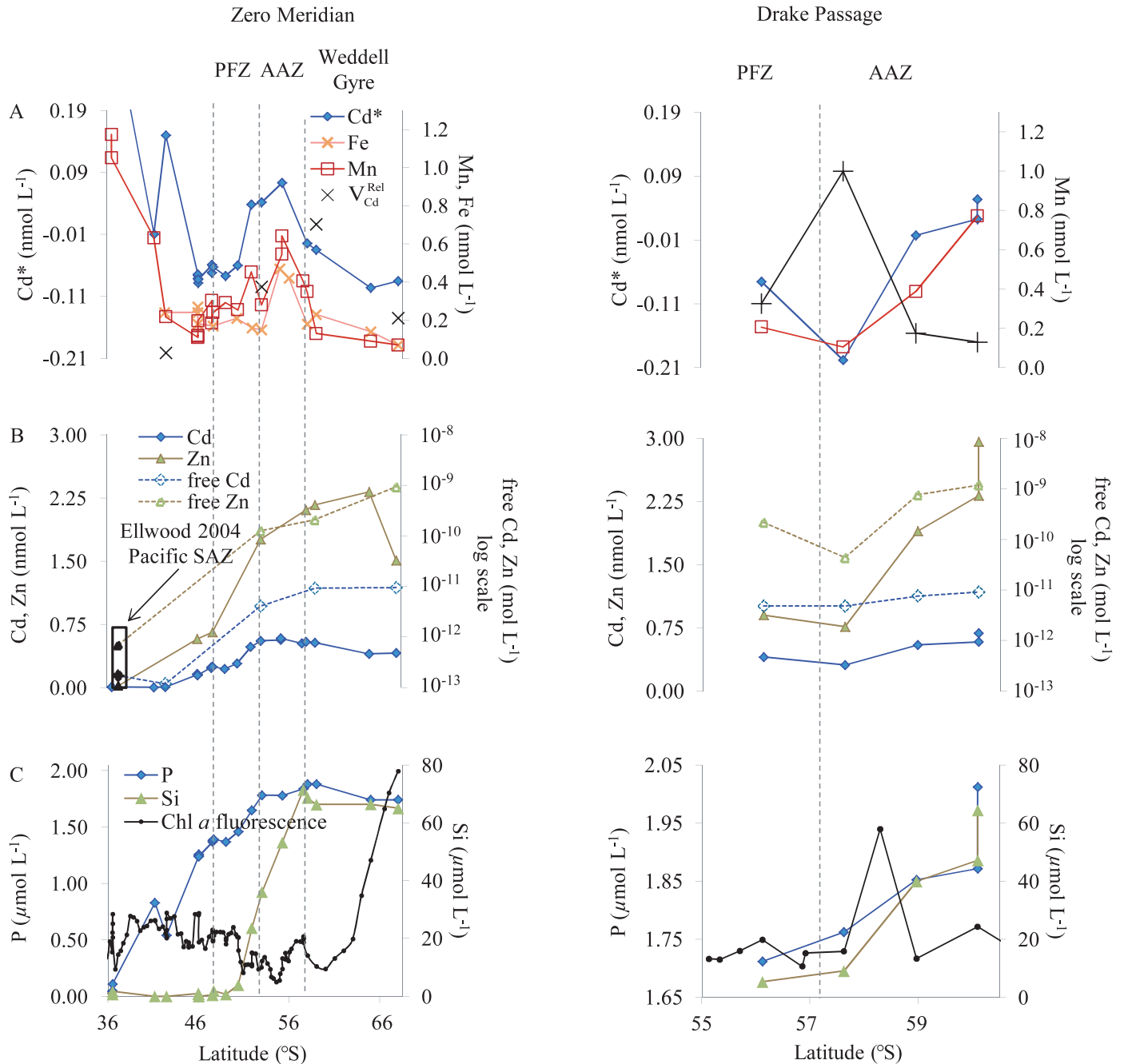
Fig. 8. Near-surface (< 60 m) sections along the Zero Meridian and the Drake Passage of (A) Cd* in comparison to Mn (Middag et al. 2011*a*, 2012), Fe (Klunder et al. 2011), and normalized Cd uptake rates V_{Cd}^{Rel} (*see* text); (B) the concentrations of Zn (Croot et al. 2011), Cd, free Cd, and free Zn (Baars and Croot 2011). Free-Cd and -Zn data from the SAZ of the East Pacific are also shown for comparison (Ellwood 2004); (C) concentrations of P, Si, and relative chlorophyll *a* fluorescence from hydrocast-mounted sensors at 35 m depth.

measurements show high Cd*, possibly related to inputs from the Antarctic Peninsula or nearby Elephant Island. While there is no evidence of riverine inputs from salinity profiles, high Cd : P could be supplied by sediment resuspension, which is also suspected to be the source for high dissolved Fe and Mn signals at this station (Middag et al. 2012). Previously reported Zn concentrations in the Drake Passage also show a peak at this station (Croot et al.

2011). However, in this context, these covariations may also point towards lower Cd : P uptake ratios in Mn-, Fe-, and potentially Zn-replete waters.

Influences on phytoplankton Cd : P uptake ratios in the Southern Ocean: It has been shown that Cd : P uptake ratios can be influenced by the bioavailability of not only Cd, but also Mn, Fe, and also Zn both in culture experiments and in the ocean (Sunda and Huntsman

2000; Cullen et al. 2003; Cullen 2005). Notably, under Fe limitation such as in the HNLC waters of the Southern Ocean, cellular Cd:P ratios are known to increase significantly (Cullen et al. 2003; Lane et al. 2009). This may be by slow growth rates or by uptake of Cd with nonspecific divalent metal transporters that may be upregulated under Fe limitation (Cullen 2006; Lane et al. 2009). Hence, higher Cd:P uptake ratios and low Cd* are expected in Fe-limited surface waters, providing a mechanistic link for a covariation of Cd* and Fe (*see* Fig. 8).

Cd may also be taken up by a low Zn-inducible uptake system under Zn-limiting conditions or with a Mn uptake system under Zn-replete conditions (Sunda and Huntsman 2000). In both cases, Cd uptake rates are correlated to the concentration of free Cd and inversely related to the concentration of free Zn. North of the APF, near-surface Zn levels are relatively low compared to Cd because of the deeper remineralization cycle of Zn, which resembles that of Si (Croot et al. 2011). This could cause high Cd uptake rates despite absolute lower concentrations of Cd compared to higher latitude stations. Due to upwelling, south of the APF, both Zn and Cd are high while Mn is low and Cd uptake is likely to occur via the Mn uptake system (Sunda and Huntsman 2000; Baars and Croot 2011). The Cd uptake rate V_{Cd} via the Mn system has been previously described by Sunda and Huntsman (2000) as:

$$V_{Cd} = \frac{V_{max}[Cd^{2+}]K_{Cd}}{[Mn^{2+}]K_{Mn} + [Cd^{2+}]K_{Cd} + [Zn^{2+}]K_{Zn} + 1} \quad (2)$$

with K_{Mn}, K_{Cd}, and K_{Zn} being the metal-binding affinities of the Mn transport system, and V_{max} being the saturation uptake rate. Using the parameters for *Thalassiosira oceanica* reported in the same paper (log K_{Mn} = 7.95; log K_{Cd} = 8.92; log K_{Zn} = 8.3), we calculate Cd uptake rates for those stations where Cd and Zn speciation as well as Mn data are available. Since Mn has been suggested to form only weak organic complexes, the bioavailable concentrations can be assumed to be proportional to total dissolved Mn (Sunda and Huntsman 2000). Speciation of Cd (this study) and Zn (Baars and Croot 2011) determined during Z&D are shown in Fig. 8 together with the calculated uptake rates relative to the highest calculated rate in this study (V_{Cd}^{Rel}), thus assuming a constant V_{max}.

At constant growth rates, the uptake rates are proportional to the Cd:P uptake ratios. For the Drake Passage, there is indeed a good inverse correlation between Cd* and V_{Cd}^{Rel}, suggesting that changes in Cd:P uptake ratios in this region may be reasonably accounted for by the model in Eq. 2. However, the changes in uptake ratios are mainly linked to variations in free Cd and free Zn, with little effect from Mn concentrations due to the lower metal binding affinity of the Mn transport system compared to those of Zn and Cd.

For the four data points along the Zero Meridian, there is also a good inverse correlation between Cd* and V_{Cd}^{Rel}, with the exception of the southernmost station which showed a very low calculated Cd uptake rate due to relatively high free Zn concentrations there. This station also exhibits the lowest Mn concentration (0.07 nmol L^{-1}). In this context, changes in Mn can affect V_{max} if Mn

concentrations occur over a range where saturation of the uptake system cannot be neglected. For example, for *T. oceanica*, an eightfold increase of V_{max} has been reported for a decrease in Mn^{2+} from 10 nmol L^{-1} to 0.5 nmol L^{-1} (Sunda and Huntsman 2000). Therefore, it is possible that the low Mn concentration at this station is associated with a significant increase in V_{max} and correspondingly higher than calculated Cd uptake rates. Our approach using Cd* also supports the interpretation of a difference in Cd isotope fractionation factors reported by Abouchami et al. (2011) towards a change from a lower affinity Mn uptake system in the AAZ where Mn and Cd* are high, to a higher affinity uptake system in the Weddell Gyre where Mn and Cd* are low. Changes in Mn uptake system affinities can therefore also represent a plausible explanation for the correlation between Cd* and Mn along the Zero Meridian.

Influences of the phytoplankton community composition on Cd:P uptake ratios: Changes in the phytoplankton community composition can have an important effect on trace metal:macro nutrient uptake ratios. North of the APF, in the PFZ and in the SAZ and STZ, nanoflagellates and dinoflagellates with reported high cellular Cd:P ratios (Ho et al. 2003) were most abundant and may contribute to the negative Cd* values in the PFZ. Surface waters south of the APF were diatom dominated, apart from B7 (62°S) in the Weddell Gyre where *Phaeocystis antarctica* was most abundant. A *P. antarctica* bloom had been observed between 61–64°S before this cruise but had subsided by the time of our study. While no near-surface sample was collected at B7, Cd* between 75–300 m showed positive values (0.043–0.079; Fig. 6), which may have resulted from remineralization of sinking cells with high cellular Cd:P (> 0.54). *P. antarctica* cells contain only soft parts and may be remineralized quickly in the upper water column and lead to this intermediate depth maximum. High Zn levels with respect to P have also been reported at this station at a depth of 300 m (Croot et al. 2011), reflecting Zn release after remineralization. This points to high Cd:P and Zn:P ratios in *P. antarctica*, which could be associated with a previously reported higher cellular N:P ratio than that of diatoms (Arrigo et al. 1999; Croot et al. 2011). Contrastingly, Lane et al. (2009) reported relatively low Cd:P ratios in a *P. antarctica* isolate compared to the diatoms *Thalassiosira pseudonana* and *T. oceanica*. The authors estimated the Cd:P ratio from Cd:C and C:P ratios using a common Redfield ratio for all phytoplankton (C:P = 106). However, it has previously been shown that *P. antarctica* in the Ross Sea have significantly higher C:P ratios (C:P = 120–154; Arrigo et al. 2002), whereas diatoms have lower C:P ratios (C:P = 76.2). Considering an additional strong increase in Cd:P uptake ratios at limiting Fe (Lane et al. 2009) and potentially Mn concentrations for *P. antarctica*, it is possible that the high Cd* values at B7 in depths between 75–300 m were related to the decay of a recent *P. antarctica* bloom.

The Cd vs. P relation in the Atlantic Ocean—Figure 9 combines the findings of this study to explain the observed Cd vs. P relation in the Atlantic Ocean and the kink in the combined Cd vs. P data set. High apparent Cd:P uptake ratios in the Southern Ocean indicate formation of particles
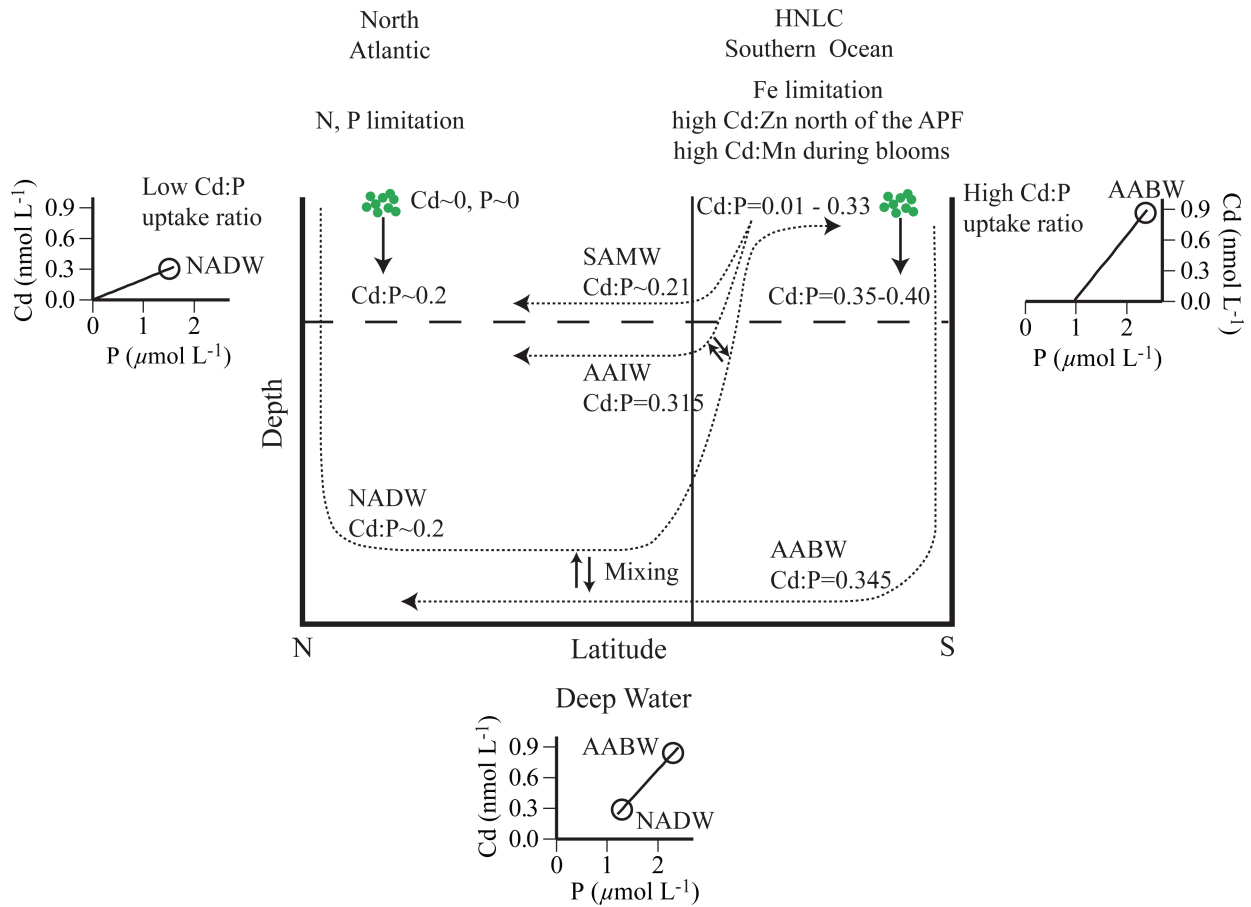
Fig. 9. Conceptual model for the formation of the observed Cd vs. P relation in the Atlantic Ocean. The North Atlantic slope and intercept is based on field studies in this area as compiled by de Baar et al. (1994). Measurements in the deep Central and South Atlantic Ocean were reported by Yeats et al. (1995).

with high Cd : P ratios, leading to Cd depletion before P in surface waters of the SAZ and a pronounced kink in the Cd vs. P relation in the Southern Ocean (*see* also Fig. 4). North of the APF, low free Zn levels relative to free Cd could cause high Cd uptake rates, despite lower concentrations of free Cd compared to stations farther south. South of the APF, both Zn and Cd were high, leading to competition for uptake sites, and uptake rates could vary depending on the local availability of Zn and Cd, whereby low Mn concentrations may also lead to higher Cd uptake rates resulting from a switch in uptake systems. Slow growth rates due to Fe limitation in addition to light limitation and cold temperatures, and increased Cd uptake with upregulated nonspecific divalent metal transporters under Fe limitation could further contribute to increase Cd : P uptake ratios in the Southern Ocean. In higher latitudes of the Southern Ocean, upwelling deep water keeps the surface dissolved Cd : P ratio at a constant level and prevents a total depletion of Cd. Upon export of the high Cd : P particles from surface waters, grazing and remineralization act to release the Cd : P content back into the dissolved phase at intermediate depth. During deep-water formation and vertical water exchange, high dissolved Cd : P ratios will eventually reach the deep Southern Ocean. Note that the Cd vs. P regression line of the deep Atlantic Ocean overlaps the regression line defined by the vertical profiles from the Southern Ocean. In the North Atlantic region, apparent Cd : P uptake ratios are lower than in the Southern Ocean and this may be related to higher Fe and Mn in this region (Moore and Braucher 2008; Middag et al. 2011b).

References

ABOUCHAMI, W., AND OTHERS. 2011. Modulation of the Southern Ocean cadmium isotope signature by ocean circulation and primary productivity. Earth Planet. Sci. Lett. **305:** 83–91.

ALDERKAMP, A. C., H. J. W. DE BAAR, R. J. W. VISSER, AND K. R. ARRIGO. 2010. Can photoinhibition control phytoplankton abundance in deeply mixed water columns of the Southern Ocean? Limnol. Oceanogr. 55: 1248–1264, doi:10.4319/lo.2010.55.3.1248

ARRIGO, K. R., D. H. ROBINSON, D. L. WORTHEN, R. B. DUNBAR, G. R. DITULLIO, M. VANWOERT, AND M. P. LIZOTTE. 1999. Phytoplankton community structure and the drawdown of nutrients and CO_2 in the Southern Ocean. Science 283: 365–367, doi:10.1126/science.283.5400.365

———, R. B. DUNBAR, M. P. LIZOTTE, AND D. H. ROBINSON. 2002. Taxon-specific differences in C/P and N/P drawdown for phytoplankton in the Ross Sea, Antarctica. Geophys. Res. Lett. 29: 441–444, doi:10.1029/2002GL015277

BAARS, O., AND P. L. CROOT. 2011. The speciation of dissolved zinc in the Atlantic sector of the Southern Ocean. Deep-Sea Res. II 58: 2720–2732, doi:10.1016/j.dsr2.2011.02.003

BLUHM, K., P. L. CROOT, O. HUHN, G. ROHARDT, AND K. LOCHTE. 2011. Distribution of iodide and iodate in the Atlantic sector of the southern ocean during austral summer. Deep-Sea Res. II 58: 2733–2748, doi:10.1016/j.dsr2.2011.02.002

BOWN, J., AND OTHERS. 2011. The biogeochemical cycle of dissolved cobalt in the Atlantic and the Southern Ocean south off the coast of South Africa. Mar. Chem. 126: 193–206, doi:10.1016/j.marchem.2011.03.008

BOYE, M., B. D. WAKE, P. L. GARCIA, J. BOWN, A. R. BAKER, AND E. P. ACHTERBERG. 2012. Distributions of dissolved trace metals (Cd, Cu, Mn, Pb, Ag) in the southeastern Atlantic and Southern Ocean. Biogeosciences 9: 3231–3246, doi:10.5194/bg-9-3231-2012

BOYLE, E. A. 1988. Cadmium: Chemical tracer of deepwater paleoceanography. Paleoceanography 3: 471–489, doi:10.1029/PA003i004p00471

BRAND, L. E., W. G. SUNDA, AND R. R. L. GUILLARD. 1986. Reduction of marine phytoplankton reproduction rates by copper and cadmium. J. Exp. Mar. Biol. Ecol. 96: 225–250, doi:10.1016/0022-0981(86)90205-4

BRULAND, K. W. 1980. Oceanographic distributions of cadmium, zinc, nickel, and copper in the North Pacific. Earth Planet. Sci. Lett. 47: 176–198.

———. 1992. Complexation of cadmium by natural organic ligands in the central North Pacific. Limnol. Oceanogr. 37: 1008–1017, doi:10.4319/lo.1992.37.5.1008

———, AND R. P. FRANKS. 1983. Mn, Ni, Cu, Zn, and Cd in the Western North Atlantic, p. 395–414. In C. S. Wong, E. Boyle, K. W. Bruland, J. D. Burton, and E. D. Goldberg [eds.], Trace metals in sea water. Plenum.

CAPODAGLIO, G., C. TURETTA, G. TOSCANO, A. GAMBARO, G. SCARPONI, AND P. CESCON. 1998. Cadmium, lead and copper complexation in Antarctic coastal seawater. Evolution during the Austral Summer. Int. J. Environ. Anal. Chem. 71: 195–226, doi:10.1080/03067319808032628

CROOT, P. L., O. BAARS, AND P. STREU. 2011. The distribution of dissolved zinc in the Atlantic sector of the Southern Ocean. Deep-Sea Res. II 58: 2707–2719, doi:10.1016/j.dsr2.2010.10.041

———, K. BLUHM, C. SCHLOSSER, P. STREU, E. BREITBARTH, R. FREW, AND M. VAN ARDELAN. 2008. Regeneration of Fe(II) during EIFeX and SOFeX. Geophys. Res. Lett. 35: L19606, doi:10.1029/2008GL035063

———, J. W. MOFFETT, AND L. BRAND. 2000. Production of extracellular Cu complexing ligands by eucaryotic phytoplankton in response to Cu stress. Limnol. Oceanogr. 45: 619–627, doi:10.4319/lo.2000.45.3.0619

CULLEN, J. T. 2005. Effects of dissolved carbon dioxide, zinc, and manganese on the cadmium to phosphorous ratio in natural phytoplankton assemblages. Limnol. Oceanogr. 50: 1193–1204, doi:10.4319/lo.2005.50.4.1193

———. 2006. On the nonlinear relationship between dissolved cadmium and phosphate in the modern global ocean: Could chronic iron limitation of phytoplankton growth cause the kink? Limnol. Oceanogr. 51: 1369–1380, doi:10.4319/lo.2006.51.3.1369

———, Z. CHASE, K. H. COALE, S. E. FITZWATER, AND R. M. SHERRELL. 2003. Effect of iron limitation on the cadmium to phosphorous ratio of natural phytoplankton assemblages from the Southern Ocean. Limnol. Oceanogr. 48: 1079–1087, doi:10.4319/lo.2003.48.3.1079

DE BAAR, H. J. W., P. M. SAAGER, R. F. NOLTING, AND J. VANDERMEER. 1994. Cadmium versus phosphate in the world ocean. Mar. Chem. 46: 261–281, doi:10.1016/0304-4203(94)90082-5

———, AND OTHERS. 2008. Titan: A new facility for ultraclean sampling of trace elements and isotopes in the deep oceans in the international Geotraces program. Mar. Chem. 111: 4–21, doi:10.1016/j.marchem.2007.07.009

DIXON, J. L., AND OTHERS. 2006. Cadmium uptake by marine micro-organisms in the English Channel and Celtic Sea. Aquat. Microb. Ecol. 44: 31–43, doi:10.3354/ame044031

ELDERFIELD, H., AND R. E. M. RICKABY. 2000. Oceanic Cd/P ratio and nutrient utilization in the glacial Southern Ocean. Nature 405: 305–310, doi:10.1038/35012507

ELLWOOD, M. J. 2004. Zinc and cadmium speciation in subantarctic waters east of New Zealand. Mar. Chem. 87: 37–58, doi:10.1016/j.marchem.2004.01.005

FAHRBACH, E., H. J. W. DE BAAR, V. C. GARÇON, AND C. PROVOST. 2011. Introduction to physics, carbon dioxide, trace elements and isotopes in the Southern Ocean: The Polarstern expeditions ANT-XXIV/3 (2008) and ANT-XXIII/3 (2006). Deep-Sea Res. II 58: 2501–2508, doi:10.1016/j.dsr2.2011.07.008

FITZWATER, S. E., K. S. JOHNSON, R. M. GORDON, K. H. COALE, AND J. W. O. SMITH. 2000. Trace metal concentrations in the Ross Sea and their relationship with nutrients and phytoplankton growth. Deep-Sea Res. II 47: 3159–3179, doi:10.1016/S0967-0645(00)00063-1

FLORENCE, T. M., AND G. E. BATLEY. 1976. Trace metal species in sea-water: Removal of trace metals from sea-water by a chelating resin. Talanta 23: 179–186, doi:10.1016/0039-9140(76)80166-X

FREW, R. D., AND K. A. HUNTER. 1992. Influence of Southern Ocean waters on the cadmium-phosphate properties of the global ocean. Nature 360: 144–146, doi:10.1038/360144a0

———, AND ———. 1995. Cadmium-phosphorous cycling at the subtropical convergence south of New Zealand. Mar. Chem. 51: 223–237, doi:10.1016/0304-4203(95)00057-7

GERRINGA, L. J. A., P. M. J. HERMAN, AND T. C. W. POORTVLIET. 1995. Comparison of the linear Van den Berg/Ruzic transformation and a non-linear fit of the Langmuir isotherm applied to Cu speciation data in the estuarine environment. Mar. Chem. 48: 131–142, doi:10.1016/0304-4203(94)00041-B

GRASSHOFF, K., K. KREMLING, AND M. EHRHARDT. 1999. Methods of seawater analysis. Wiley-VCH.

GRZYBOWSKI, W. 2000. Comparison between stability constants of cadmium and lead with humic substances of different molecular weight isolated from Baltic Sea water. Oceanologia 42: 473–482.

HO, T. Y., A. QUIGG, Z. V. FINKEL, A. J. MILLIGAN, K. WYMAN, P. G. FALKOWSKI, AND F. M. M. MOREL. 2003. The elemental composition of some marine phytoplankton. J. Phycol. 39: 1145–1159, doi:10.1111/j.0022-3646.2003.03-090.x

KLUNDER, M. B., P. LAAN, R. MIDDAG, H. J. W. DE BAAR, AND J. V. OOIJEN. 2011. Dissolved iron in the Southern Ocean (Atlantic sector). Deep-Sea Res. II 58: 2678–2694, doi:10.1016/j.dsr2.2010.10.042

KOZELKA, P. B., AND K. W. BRULAND. 1998. Chemical speciation of dissolved Cu, Zn, Cd, Pb in Narragansett Bay, Rhode Island. Mar. Chem. **60:** 267–282, doi:10.1016/S0304-4203(97)00107-2

KREMLING, K., J. PIUZE, K. BRÖCKEL, AND C. S. WONG. 1978. Studies on the pathways and effects of cadmium in controlled ecosystem enclosures. Mar. Biol. **48:** 1–10. , doi:10.1007/BF00390525

KUIPER, J. 1981. Fate and effects of cadmium in marine plankton communities in experimental enclosures. Mar. Ecol. Prog. Ser. **6:** 161–174, doi:10.3354/meps006161

LAGLERA, L. M., AND C. M. G. VAN DEN BERG. 2006. Photo-chemical oxidation of thiols and copper complexing ligands in estuarine waters. Mar. Chem. **101:** 130–140, doi:10.1016/j.marchem.2006.01.006

LANE, E. S., D. M. SEMENIUK, R. F. STRZEPEK, J. T. CULLEN, AND M. T. MALDONADO. 2009. Effects of iron limitation on intracellular cadmium of cultured phytoplankton: Implications for surface dissolved cadmium to phosphate ratios. Mar. Chem. **115:** 155–162, doi:10.1016/j.marchem.2009.07.008

LE MOIGNE, F. A. C., M. BOYE, A. MASSON, R. CORVAISIER, E. GROSSTEFFAN, A. GUENEUGUES, AND P. PONDAVEN. 2013. Description of the biogeochemical features of the subtropical southeastern Atlantic and the Southern Ocean south of South Africa during the austral summer of the International Polar Year. Biogeosciences **10:** 281–295, doi:10.5194/bg-10-281-2013

LEE, J. G., B. A. AHNER, AND F. M. M. MOREL. 1996. Export of cadmium and phytochelatin by the marine diatom *Thalassiosira weissflogii*. Environ. Sci. Technol. **30:** 1814–1821, doi:10.1021/es950331p

LÖSCHER, B. M., J. T. M. DE JONG, AND H. J. W. DE BAAR. 1998. The distribution and preferential biological uptake of cadmium at 6°W in the Southern Ocean. Mar. Chem. **62:** 259–286, doi:10.1016/S0304-4203(98)00045-0

———, J. VAN DER MEER, H. J. W. DE BAAR, P. M. SAAGER, AND J. T. M. DE JONG. 1997. The global Cd/phosphate relationship in deep ocean waters and the need for accuracy. Mar. Chem. **59:** 87–93, doi:10.1016/S0304-4203(97)00067-4

MARTIN, J. H., S. E. FITZWATER, R. M. GORDON, C. N. HUNTER, AND S. J. TANNER. 1993. Iron, primary production and carbon nitrogen flux studies during the Jgofs North-Atlantic Bloom Experiment. Deep-Sea Res. II **40:** 115–134, doi:10.1016/0967-0645(93)90009-C

———, R. M. GORDON, AND S. E. FITZWATER. 1990. Iron in Antarctic waters. Nature **345:** 156–157, doi:10.1038/345156a0

MIDDAG, R., H. J. W. DE BAAR, P. LAAN, P. H. CAI, AND J. C. VAN OOIJEN. 2011a. Dissolved manganese in the Atlantic sector of the Southern Ocean. Deep-Sea Res. II **58:** 115–134.

———, ———, ———, AND O. HUHN. 2012. The effects of continental margins and water mass circulation on the distribution of dissolved aluminum and manganese in Drake Passage. J. Geophys. Res. : Oceans **117:** C01019, doi:10.1029/2011JC007434

———, ———, ———, AND M. B. KLUNDER. 2011b. Fluvial and hydrothermal input of manganese into the Arctic Ocean. Geochim. Cosmochim. Acta **75:** 2393–2408, doi:10.1016/j.gca.2011.02.011

MOORE, J. K., AND O. BRAUCHER. 2008. Sedimentary and mineral dust sources of dissolved iron to the world ocean. Biogeosciences **5:** 631–656, doi:10.5194/bg-5-631-2008

MURPHY, J., AND J. P. RILEY. 1962. A modified single solution method for determination of phosphate in natural waters. Anal. Chim. Acta **27:** 31–36, doi:10.1016/S0003-2670(00)88444-5

NOLTING, R. F., AND H. J. W. D. BAAR. 1994. Behaviour of nickel, copper, zinc and cadmium in the upper 300 m of a transect in the Southern Ocean (57°–62°S, 49°W). Mar. Chem. **45:** 225–242, doi:10.1016/0304-4203(94)90006-X

PAKHOMOV, E. A., R. PERISSINOTTO, C. D. MCQUAID, AND P. W. FRONEMAN. 2000. Zooplankton structure and grazing in the Atlantic sector of the Southern Ocean in late austral summer 1993—part 1. Ecological zonation. Deep-Sea Res. I **47:** 1663–1686, doi:10.1016/S0967-0637(99)00122-3

PRICE, N. M., AND F. M. M. MOREL. 1990. Cadmium and cobalt substitution for zinc in a marine diatom. Nature **344:** 658–660, doi:10.1038/344658a0

SANDER, S. G., A. KOSCHINSKY, G. MASSOTH, M. STOTT, AND K. A. HUNTER. 2007. Organic complexation of copper in deep-sea hydrothermal vent systems. Environ. Chem. **4:** 81–89, doi:10.1071/EN06086

SARMIENTO, J. L., N. GRUBER, M. A. BRZEZINSKI, AND J. P. DUNNE. 2004. High-latitude controls of thermocline nutrients and low latitude biological productivity. Nature **427:** 56–60, doi:10.1038/nature02127

———, J. SIMEON, A. GNANADESIKAN, N. GRUBER, R. M. KEY, AND R. SCHLITZER. 2007. Deep ocean biogeochemistry of silicic acid and nitrate. Global Biogeochem. Cycles **21:** GB1S90, doi:10.1029/2006GB002720

SCHLITZER, R. 2013. Ocean Data View [Internet]. Bremerhaven, Germany: Alfred-Wegener-Institute [accessed 05 March 2013], Available from http://odv.awi.de

SCHMITT, A. D., S. J. G. GALER, AND W. ABOUCHAMI. 2009. High-precision cadmium stable isotope measurements by double spike thermal ionisation mass spectrometry. J. Anal. At. Spectrom. **24:** 1079–1088, doi:10.1039/b821576f

SKRABAL, S. A., K. L. LIESEKE, AND R. J. KIEBER. 2006. Dissolved zinc and zinc-complexing ligands in an organic-rich estuary: Benthic fluxes and comparison with copper speciation. Mar. Chem. **100:** 108–123, doi:10.1016/j.marchem.2005.12.004

SUNDA, W. G., AND S. A. HUNTSMAN. 2000. Effect of Zn, Mn, and Fe on Cd accumulation in phytoplankton: Implications for oceanic Cd cycling. Limnol. Oceanogr. **45:** 1501–1516, doi:10.4319/lo.2000.45.7.1501

TREGUER, P., AND P. LECORRE. 1979. Ratios of nitrate, phosphate, and silicate during uptake and regeneration phases of the Maroccan Upwelling Regime. Deep-Sea Res. I **26:** 163–184.

WEI, L., AND B. A. AHNER. 2005. Sources and sinks of dissolved phytochelatin in natural seawater. Limnol. Oceanogr. **50:** 13–22, doi:10.4319/lo.2005.50.1.0013

WESTERLUND, S., AND P. ÖHMAN. 1991. Cadmium, copper, nickel, lead, and zinc in the water column of the Weddell Sea, Antarctica. Geochim. Cosmochim. Acta **55:** 2127–2146, doi:10.1016/0016-7037(91)90092-J

YANG, S.-C., D.-C. LEE, AND T.-Y. HO. 2012. The isotopic composition of cadmium in the water column of the South China Sea. Geochim. Cosmochim. Acta **98:** 66–77, doi:10.1016/j.gca.2012.09.022

YEATS, P. A. 1998. An isopycnal analysis of cadmium distributions in the Atlantic Ocean. Mar. Chem. **61:** 15–23, doi:10.1016/S0304-4203(98)00004-8

———, S. WESTERLUND, AND A. R. FLEGAL. 1995. Cadmium, copper and nickel distributions at four stations in the eastern central and south Atlantic. Mar. Chem. **49:** 283–293, doi:10.1016/0304-4203(95)00018-M